Hindawi
Advances in Civil Engineering
Volume 2022, Article ID 1970591, 10 pages
https://doi.org/10.1155/2022/1970591

Research Article

Experimental Study on Dynamic Compression Mechanics of Sandstone after Coupled Alkali-Chemical-Dynamic Interaction

Qi Ping,[1,2,3] **Chen Wang**,[2,3] **Qi Gao**,[2,3] **Kaifan Shen**,[2,3] **Yulin Wu**,[2,3] **Shuo Wang**,[2,3] **and Xiangyang Li**[2,3]

[1]*State Key Laboratory of Mining Response and Disaster Prevention and Control in Deep Coal Mine, Anhui University of Science and Technology, Huainan, Anhui 232001, China*
[2]*Research Center of Mine Underground Engineering, Ministry of Education, Anhui University of Science and Technology, Huainan, Anhui 232001, China*
[3]*School of Civil Engineering and Architecture, Anhui University of Science and Technology, Huainan, Anhui 232001, China*

Correspondence should be addressed to Qi Ping; ahpingqi@163.com

Received 4 July 2022; Accepted 20 September 2022; Published 10 October 2022

Academic Editor: Quan Jiang

For the purpose of analyzing the effect of the alkaline solutions on the mechanical property of sandstone impact compression, the sandstone specimens of coal mine roadway were corroded in NaOH solution with pH 7 (neutral pure water solution) and pH = 8, 9, 10, 11, and 12 for 28 d, followed by dynamic compression tests using a separated Hopkinson compression bar test device, and the microstructural changes of the specimens were measured by SEM electron microscope scanning equipment. The studies indicate that the degree of damage to the dynamic properties of a sandstone specimen is tightly correlated with the variation of the pH value of the corrosion solution. The corrosion deterioration effect of the strong alkaline solution is most obvious, followed by the weak alkaline solution, and the mechanical properties of the sandstone are relatively stable under a neutral solution. The dynamic compressive strength and dynamic modulus of elasticity of specimens decrease as a quadratic and cubic function, respectively, with the rising pH of the solution. The dynamic peak strain and average strain rate tend to increase with the increase in pH, and they are larger than those of the uncorroded specimens. As the pH of the solution rises, the impact damage of the sandstone specimens intensifies, and the average particle size of the fragments tends to decrease in a quadratic polynomial.

1. Introduction

Due to the continuous development of the world economy and modern engineering industry, both the development of mineral resources such as deep oil and natural gas and the deep burial disposal of highly radioactive nuclear waste, as well as the construction of rock works such as tunnels and water conservancy projects, are increasing [1]. The stability of underground rock engineering is usually affected by high ground pressure, high seepage flow [2], and high ground temperature [3]. And the influence of corrosion damage of groundwater on deep underground engineering has attracted the attention of many scholars in recent years, and studies related to static tests of different kinds of rocks under the action of water-rock chemistry have been carried out. Li et al. [4] utilized the rock mass AE technology to study the uniaxial compression destruction degree of red-bedded soft rocks after being subjected to different acidic pH chemical solutions. Fu et al. [5] used different pH solutions to soak rock samples to explore the effect law of chemical solutions on mechanical properties as well as corrosion mechanism of brilliant rocks for the mining difficulties caused by the intrusion of dense and hard brilliant rocks into coal seams. Huo et al. [6] combined the uniaxial compression test and CT scan test to analyze the basic physical characteristics as well as mechanical property changes of sandstone corroded by acidic solutions. Ding et al. [7] conducted mechanical tests on Longmen Grottoes tuff under different chemical solutions and studied both the strength damage characteristics and solubility properties. Ling et al. [8] conducted

nonequilibrium flow dynamic corrosion tests on black shale immersed in acidic aqueous solutions with different pH and analyzed its deformation and strength characteristic at different deformation and strength characteristics patterns during different soaking periods. Miao et al. [9] carried out static compression mechanical experiments and splitting experiments on marble after soaking in different acidic NaCl solutions, comparing and analyzing the strength deterioration, axial deflection characteristics, and destructive effects of mechanical properties and parameters of granite under different acidic chemical environments. Shen et al. [10] completed a triaxial creep experiment in single fissure granite with simultaneous chemical solution percolation. The comprehensive response mechanism of single fissure rocks under a stress-percolation-chemical coupling environment was studied. Zhou and Chen [11] conducted uniaxial mechanical tests and electron microscope scanning test analysis of granite under different times of erosion by different acidic solutions. Yuan et al. [12] investigated sandstone under the fundamentals of chemical thermodynamics and chemical dynamics. In addition, the energy evolution and damage characteristics of fractured carbonaceous shale subjected to dry-wet circulations were studied. Liu et al. [13] made intact and fissure dip angles of 30°, 45°, and 60° charcoal shale and subjected them to triaxial compression tests under different dry-wet circulations to investigate their effects on the strength, destruction mode, and energy evolution of single fissure charcoal shale.

The surrounding rocks of underground projects are not only eroded by water-chemical solutions but also bear dynamic loads such as mechanical digging, blasting excavation, and seismic impact at the same time [14], which leads to hidden problems in the construction and stability of rock works. It can be seen that the dynamics of the rock is also an important influence on the stability performance and safety performance in underground rock engineering. While the separated Hopkinson compression bar test device is widely used in the tests related to rock dynamic mechanics, Ping et al. [15] studied the problem of how to select a reasonable loading waveform in SHPB experiment. Li et al. [16] investigated the energy dissipation in the impact splitting test of prefabricated single-nodular rock under high strain rate. Yuan and Ma [17] analyzed the influence of water content on the kinetic properties in sandstone after SHPB uniaxial compression test.

There are relatively few tests on rock mechanics under coupled chemical-dynamic conditions. Li et al. [18] conducted impact compression experiments on limestone under erosion in 3 sets of different pH solutions to study its dynamic mechanical properties. Zhang et al. [19] investigated a dynamic tensile mechanical characteristic of limestone with different times of corrosion by the same acidic solution. Li et al. [20] carried out dynamic tensile tests on chert under corrosion in three groups of different acidic solutions and investigated the relationship between dynamic tensile strength and specific energy in the specimens. Ping et al. [21] analyzed the kinetic property changes of the roadway sandstone under different days of corrosion by strong alkali solutions.

Groundwater is generally alkaline, and underground rockworks are subjected to dynamic load impact damage effects in addition to experiencing prolonged corrosion damage by the water-chemical environment [22]. To research the influence of alkaline solution erosion on the dynamic compression characteristics of sandstone, the tests in this study configured NaOH solutions of pH 7, 8, 9, 10, 11, and 12 and placed the sandstone specimens in them for 28 days. Finally, impact compression tests were performed on sandstone specimens at a constant loading rate using a 50 mm diameter split Hopkinson compression bar experimental setup. Several dynamic mechanical parameters of sandstone specimens as well as the microlevel corrosion conditions were analyzed and summarized as influenced by the pH change of the water chemical solution.

2. Sandstone Specimen Preparation and Impact Compression Test Procedure

2.1. Corrosion Specimen Preparation. The specimens used in this study were obtained from sandstone of the roadway of the Gu Bei coal mine in Huainan City, which had a greyish-white surface.

To increase the homogeneity of the test, the sandstone samples selected for the test were obtained from identical rock. X-ray diffraction (XRD) tests were then performed, and the mineral composition of the rock samples has been analyzed against standard PDF cards. The main components were quartz (SiO_2), albite (Na (Si_3Al) O_8), and kaolinite ($Al_2Si_2O_5$ (OH) $_4$), and the molecular formulas of the other minor constituent minerals were Al_2O_3, Fe_2O_3, CaO, Na_2O, K_2O, and MgO. The diffraction energy spectrum is shown in Figure 1.

In accordance with the requirements of the rock dynamic properties test protocol [23], the rock has been made into standard specimens of 50 mm in diameter and 25 mm in height through three processes of coring, cutting, and grinding, and control the specimen size error within ±2 mm, the two end surface unevenness error of ±0.05 mm, and the axis allowable error of ±0.25° [24]. Twenty one specimens were made in total and 3 were selected as uncorroded specimens, while the other 18 have been classified into six sets and subjected to corrosion tests with different pH solutions.

Six sets of aqueous chemical solutions with pH 7, 8, 9, 10, 11, and 12 were used in the experiment, as indicated in Figure 2. Each group of the chemical solution was put into 3 specimens for corrosion, and the corrosion time was 28 d. PHS-25 digital display acidity meter was used to measure the pH variation of its solution regularly every day, and all specimens were removed from the solution after the corrosion test.

2.2. Dynamical Test Device. The SHPB experimental equipment used for the impact compression test was provided by the State Key Laboratory of Mining Response and Disaster Prevention and Control in Deep Coal Mines, which is indicated in Figure 3.

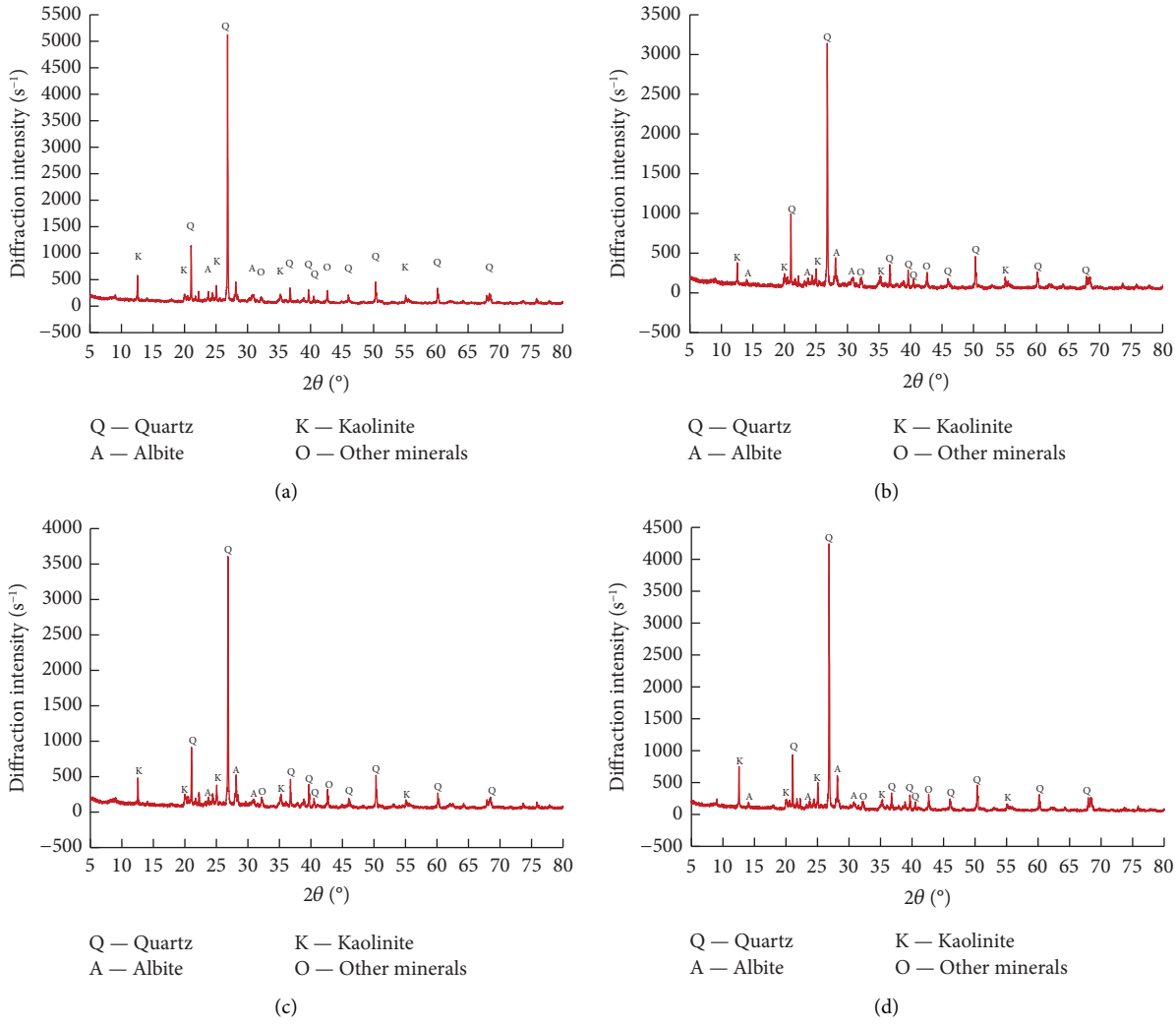

Figure 1: X-ray diffraction spectrum. (a) Uncorroded. (b) pH=7. (c) pH=9. (d) pH=12.

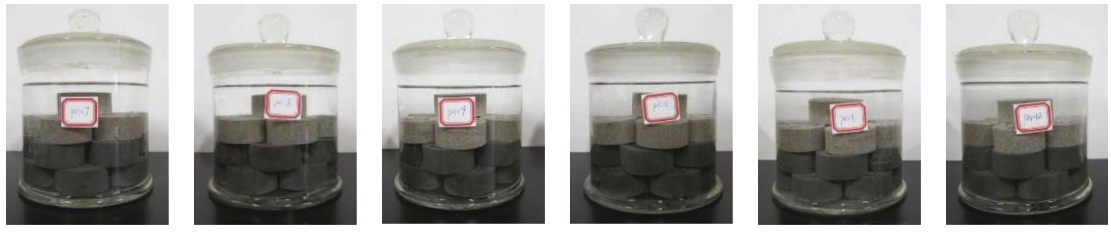

Figure 2: Sandstone corroded specimen. (a) pH=7; (b) pH=8; (c) pH=9; (d) pH=10; (e) pH=11; (f) pH=12.

Figure 3: SHPB experimental equipment.

The material of the rods is all high-strength 40Cr alloy steel, whose longitudinal wave speed is 5190 m/s. The incident and transmission rods are 2000 mm and 1500 mm long, respectively, and both have a 50 mm diameter. The high-pressure nitrogen gas is released instantaneously to drive the spindle-shaped bullet impact rod to move at a high speed for impact loading. In addition, an appropriate amount of vaseline was applied to both ends of the specimen to reduce the end-face friction effect.

Based on the fundamental of impact dynamic experiment [25], the three-wave method was used to process all data obtained from the data acquisition system [26], so as to calculate the relevant kinetic indicators such as stress $\sigma(t)$, strain $\varepsilon(t)$, and strain rate $\varepsilon(t)$ of the rock specimen. The calculation principle is indicated as

$$\left.\begin{aligned}\sigma(t) &= \frac{E_0 A_0}{2A_S}\left[\varepsilon_I(t) + \varepsilon_R(t) + \varepsilon_T(t)\right] \\ \varepsilon(t) &= \frac{C_0}{L_S}\int_0^T \left[\varepsilon_I(t) + \varepsilon_R(t) - \varepsilon_T(t)\right]\mathrm{d}t \\ \varepsilon(t) &= \frac{C_0}{L_S}\left[\varepsilon_I(t) + \varepsilon_R(t) - \varepsilon_T(t)\right]\end{aligned}\right\}, \quad (1)$$

where A_0 and A_S represent the cross-sectional areas of compression bar and specimen. $\varepsilon_I(t)$, $\varepsilon_R(t)$, and $\varepsilon_T(t)$ represent the incident stress wave, reflected stress wave, and transmitted stress wave in the moment t, respectively. E_0 and C_0 represent the modulus of elasticity of the compression bar and the longitudinal wave speed. L_S represent the length of the specimen; t is the continuation time of the stress wave.

2.3. Solution pH Variation. Starting from the immersion of all sandstone specimens into the solution, the pH change of the solution was measured regularly every day using a PHS-25 digital display acidity meter, and the pH change curve of each solution with time is shown in Figure 4.

As shown in Figure 5, the pH of the strong alkali solution (pH = 11, 12) decreases continuously and tends to be neutral as the corrosion time increases; the pH of the weak alkali solution (pH = 8) increases slightly; the solutions with pH of 9 and 10 change less and level out; while the pH of neutral pure water decreases slightly and tends to be weakly acidic. Compared with the weak alkali solution, the concentration of OH^- in the strong alkali solution is higher, and the chemical reaction rate with sandstone mineral components is faster and more fully reacted, resulting in the consumption of OH^- in the strong alkali solution which is much larger than that in weak alkali solution; thus, its pH decreases significantly. In addition, the pH change of each solution has a time effect. During the pre-water-rock chemistry phase, some mineral components in sandstone react chemically with OH^- in solution or hydrolyze with solution, accompanied by the consumption of original substances and the generation of precipitation and other substances, which leads to a more significant change of solution pH, and during the late stage of water-rock action, due to the continuous consumption of some mineral components in sandstone, the chemical reaction rate decreases; thus, the change of solution pH is relatively small and tends to level off gradually.

With reference to the previous studies [27–30] and combined with the mineral composition of sandstone obtained from XRD tests, the equations of water-rock chemical reactions occurring in different water chemical solutions tested in this study can be summarized as follows.

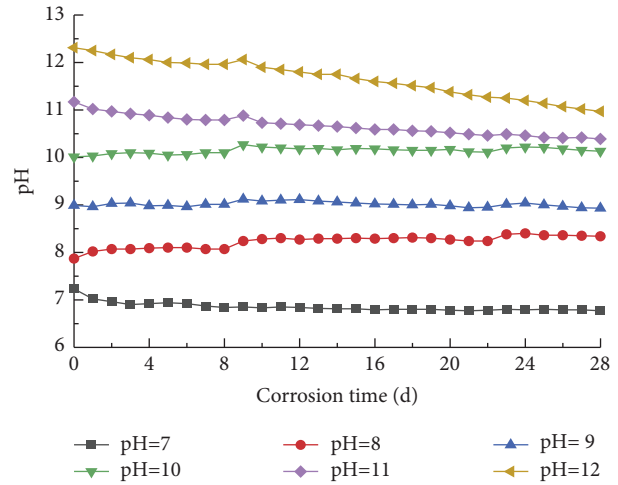

Figure 4: Curves of pH value variation with time in hydrochemical solutions.

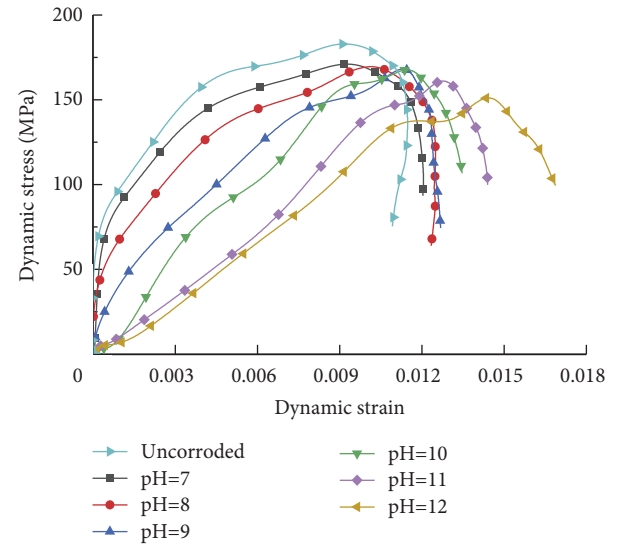

Figure 5: Dynamic stress-strain curves on sandstone specimens under erosion with different pH solutions.

The hydrolysis reactions of some mineral components of sandstone in neutral pure water solutions occur as shown in equations (2)–(6):

$$SiO_2 + 2H_2O \longrightarrow H_3SiO_4^- + H^+ \quad (2)$$

$$Na(Si_3Al)O_8 + 8H_2O \longrightarrow Na^+ + Al(OH)_4^- + 3H_4SiO_4 \quad (3)$$

$$MgO + H_2O \longrightarrow Mg(OH)_2 \quad (4)$$

$$Na_2O + H_2O \longrightarrow 2Na^+ + 2OH^- \quad (5)$$

$$K_2O + H_2O \longrightarrow 2K^+ + 2OH^- \quad (6)$$

The main chemical reactions occurring in alkaline solutions with sandstone mineral components are shown in (10):

$$SiO_2 + 2OH^- \longrightarrow SiO_3^{2-} + H_2O \quad (7)$$

$$Al^{3+} + 3OH^- \longrightarrow Al(OH)_3\downarrow \quad (8)$$

$$Ca^{2+} + 2OH^- \longrightarrow Ca(OH)_2\downarrow \quad (9)$$

$$Al_2Si_2O_5(OH)_4 + 6OH^- + H_2O \longrightarrow 2Al(OH)_4^- + 2SiO_2(OH)_4^{2-}. \quad (10)$$

In addition to the above chemical reaction equations, water-rock chemistry also includes dissolution and dissolution, which will likewise lead to an increase in the degree of microscopic chemical damage in sandstone specimens, thus causing different degrees of deterioration in their dynamic mechanical properties.

3. Experimental Discussion and Analysis

3.1. Sandstone Dynamic Stress-Strain Variation. A dynamic compression test was carried out under a shock air pressure of 0.50 MPa, and the dynamic stress-strain curves of sandstone specimens were without corrosion and after corrosion with different pH solutions (see Figure 5).

According to the analysis, the dynamic mechanical properties in specimens show a deterioration trend after erosion by different pH solutions, and the greatest decrease in dynamic compressive strength is after erosion by a strong alkali solution, and the corresponding breaking strain increases sharply, followed by corrosion by a weak alkali solution, while the smallest decrease in dynamic compressive strength is after erosion by a neutral solution. After preliminary analysis, the pH value is a significant factor affecting the variation of dynamic mechanical parameters of the rock.

Figures 6 and 7 and Table 1 show the variation of dynamic compressive strength and the dynamic peak strain for the specimens under different pH solution conditions.

The results obtained showed that σ_d for the uncorroded specimens was up to 183.67 MPa. However, σ_d of the sandstone specimens showed a quadratic decreasing trend after 28 d of corrosion treatment by six pH solutions, in which the strength of the specimens decreased the least by 6.58% after corrosion by neutral solution, while the maximum decrease was 17.11% at pH 12. The corresponding ε_d of the sandstone specimens had an increase of 21.34%, 35.30%, 42.15%, 49.99%, 53.14%, and 82.01%, respectively, compared with the uncorroded sandstone specimens. Clearly, the growth of ε_d of sandstone specimens under the corrosion of neutral and weak alkaline solutions is relatively small, and the growth of ε_d increases gradually as the alkalinity increases, reaching its peak under the corrosion of strong alkaline solutions with pH 12. This is because some of the constituent minerals decompose and produce precipitation and other substances after chemical reaction under an alkaline solution, which leads to the destruction of the original internal structure and the expansion and increase of the number of microcracks again, thus showing the deterioration of σ_d and the increase of ε_d amplitude.

3.2. Variation of Dynamic Modulus of Elasticity and Average Strain Rate. The changes in modulus of dynamic elasticity as well as average strain-rate of the specimens corroded by different pH solutions are shown in Figures 8 and 9, respectively.

From Figure 8, E_d decreases with increasing pH in a cubic function, and the higher the pH of the solution, the greater the decrease. Moreover, the percentage loss of E_d value was 5.12%, 5.73%, 6.48%, 13.95%, 18.84%, and 38.45% after corrosion of specimens with different pH solutions compared with uncorroded specimens. The reasons are as follows. As the pH value increases, the solution erosion effect is enhanced, and the internal microcracks of sandstone specimens are extended continuously, leading to a gradual decrease of the resistance to deformation of sandstone specimens, and the deterioration of impact mechanical characteristics of specimens in strong alkaline solution corrosion is more obvious compared with neutral pure water solution and weak alkaline solution.

From Figure 9, $\dot{\varepsilon}$ showed a quadratic polynomial positive correlation with increasing pH of the solution, as well as the higher the pH, the larger the rise in $\dot{\varepsilon}$. Moreover, the $\dot{\varepsilon}$ rise values were 1.04%, 3.42%, 10.80%, 20.03%, 28.38%, and 63.78% after the corrosion of specimens with different pH solutions compared with the uncorroded specimens. It can be observed that the variation in $\dot{\varepsilon}$ of sandstone after corrosion in a neutral solution is small and can be neglected, while in an alkaline solution, σ_d decreases, as well as $\dot{\varepsilon}$ rises as pH increases, which represents a more significant strain-rate effect.

3.3. Corrosion Microscopic Damage Mechanism of Sandstone Specimens. Figure 10 shows the SEM electron microscope scanning test images of the specimens under the corrosion of different pH solutions.

As it is observed in Figure 10, uncorroded sandstone is structurally dense with occasional secondary pores. While in neutral pure water solution, sandstone undergoes just a little hydrolytic reaction, making the specimen porous. While in the alkaline surface is relatively smooth, the degree of deterioration damage is small. In an alkaline solution, sodium feldspar and other major mineral components in sandstone react with OH^- to produce free K^+ and Na^+, while a small amount of Al^{3+} and Ca^{2+} combine with OH^- to produce a white precipitate, which can be observed in SEM images as a little white crystal on the surface of sandstone specimens. And in alkaline solutions with different pH solutions, the intensity of chemical reactions occurring varies. It can be

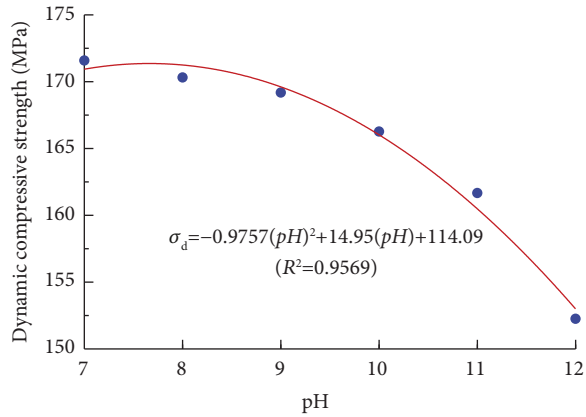

Figure 6: Relationship between dynamic compressive strength and pH.

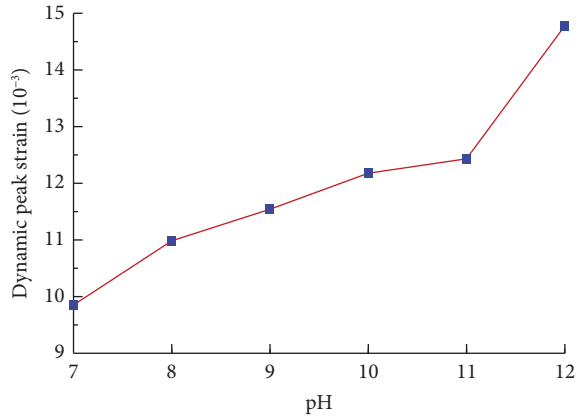

Figure 7: Relationship between dynamic peak strain and pH.

Table 1: Selected dynamic mechanical parameters of some corrosion specimens.

pH	Specimen number	Dynamic compressive strength σ_d (MPa)	Dynamic peak strain $\varepsilon_d/10^{-3}$	Dynamic modulus of elasticity E_d (GPa)	Average strain rate $\dot{\varepsilon}(s^{-1})$
Uncorroded	GB41-19	183.67	8.118	18.463	66.654
7	GB41-03	171.59	9.850	17.518	67.243
8	GB41-06	170.32	10.983	17.404	68.829
9	GB41-07	169.19	11.540	17.267	73.744
10	GB41-12	166.27	12.176	15.888	79.885
11	GB41-13	161.66	12.432	14.985	85.436
12	GB41-17	152.25	14.776	11.365	109.001

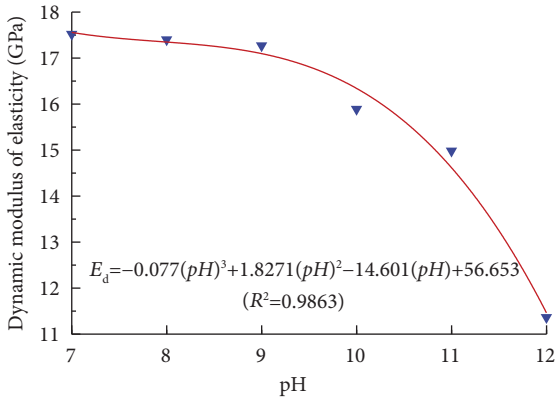

Figure 8: Relationship between dynamic elastic modulus and pH.

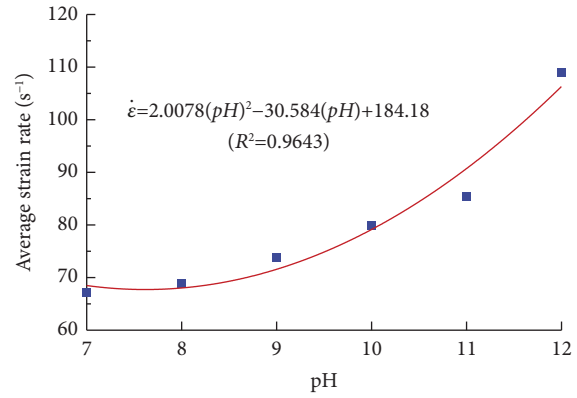

Figure 9: Relationship between average strain rate and pH.

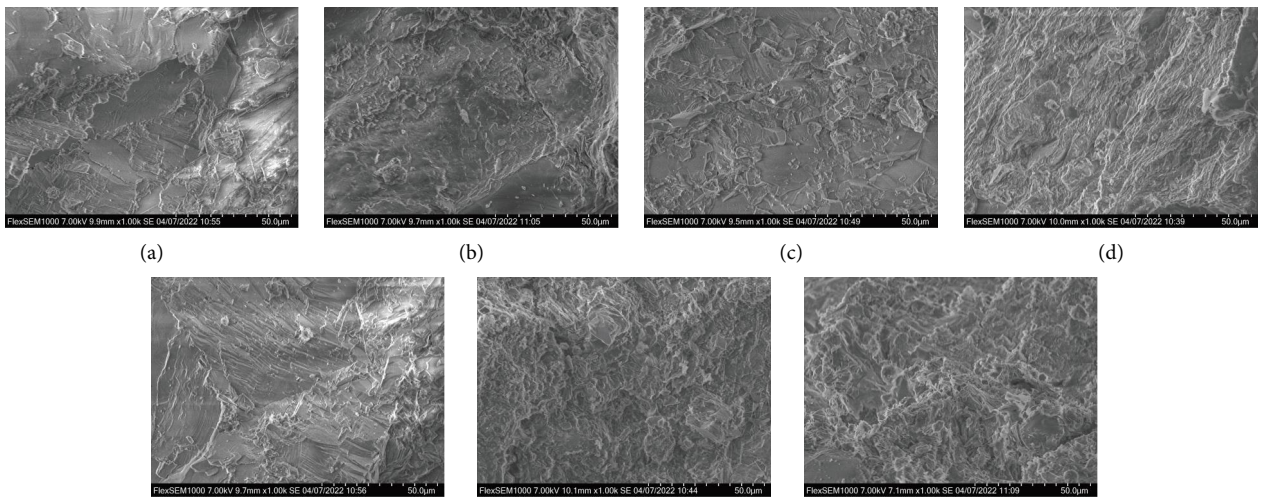

Figure 10: SEM images of specimens after corrosion in various pH solutions. (a) Uncorroded. (b) pH=7 (c) pH=8. (d) pH=9. (e) pH=10. (f) pH=11. (g) pH=12.

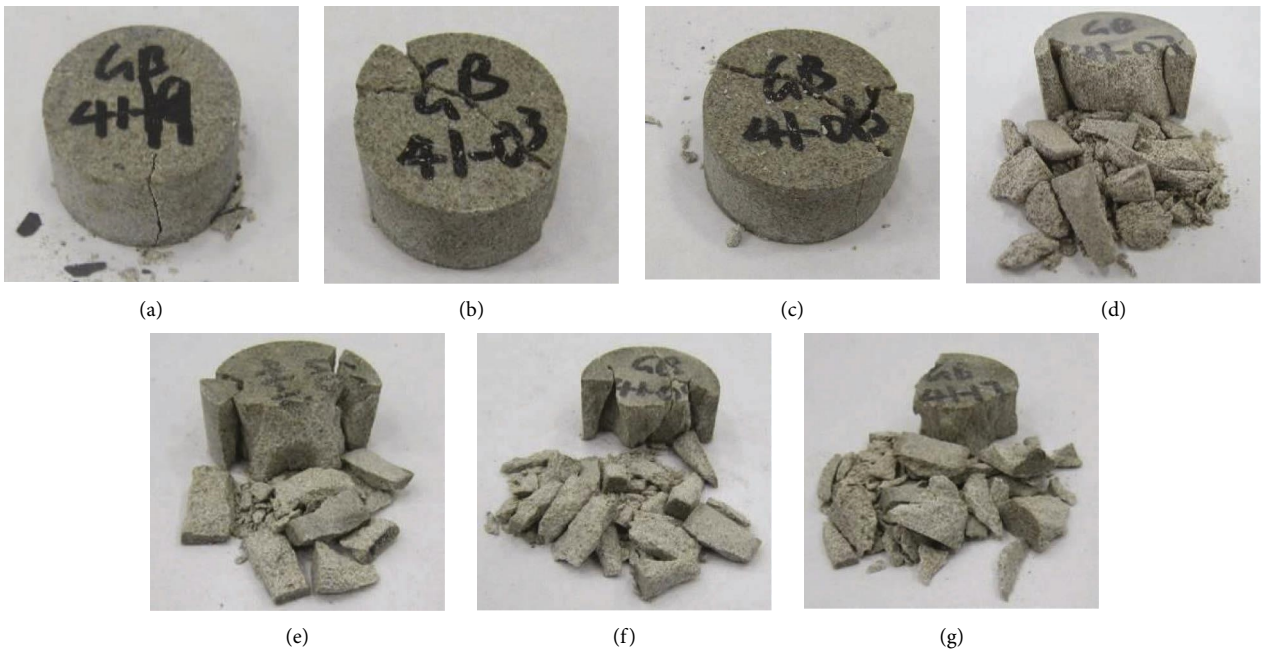

Figure 11: Impact damage forms of sandstone corroded by different pH solutions. (a) Uncorroded. (b) pH=7. (c) pH=8. (d) pH=9. (e) pH=10. (f) pH=11. (g) pH=12.

observed that microcracks in the internal structure of sandstone start to expand after soaking in neutral solutions, and a small amount of microporosity appears in sandstone in weakly alkaline solutions. With the enhancement of alkalinity, the corrosion phenomenon on the surface of the specimen becomes more and more serious, and the number of secondary pores and microcracks inside gradually increases, no longer maintaining the original compact structure. Therefore, the degree of sandstone damage caused by erosion of strong alkali solutions is greatest, followed by weak alkali solutions, and the neutral solution is the least, which is corroborated with the previous law that the deterioration of dynamic mechanical properties increases with the increasing pH value.

3.4. Specimen Impact Damage Forms. As it is observed in Figure 11, compared with the uncorroded specimens, the sandstone specimens were less damaged after corrosion by neutral and weak alkaline solutions, as well as the broken form was characterized by the basic integrity of the specimen surface and the presence of fragments of larger size, accompanied by a small amount of debris. As the pH value of the corrosion solution rose from 9 to 12, it was observed that

Table 2: Sieving results of sandstone specimens in broken pieces.

pH	Number	Diameter of sieve hole (mm)									Total mass (g)	Average particle size of fragments (mm)
		0.15	0.3	0.6	1.18	2.36	4.75	9.5	13.2	16.0		
7	GB41-03	0.21	0.18	0.30	0.25	0.35	0.90	3.71	4.53	115.62	126.05	15.47
8	GB41-06	0.17	0.15	0.32	0.30	0.26	3.48	4.20	0.00	121.80	130.68	15.35
9	GB41-07	0.56	0.54	0.81	0.86	1.23	3.25	10.22	4.18	105.08	126.73	14.63
10	GB41-12	0.78	0.75	1.34	1.39	3.41	8.81	7.04	10.69	88.83	123.04	13.67
11	GB41-13	1.24	1.05	1.64	1.58	2.73	10.98	15.94	19.72	71.15	126.03	12.79
12	GB41-17	2.16	1.89	2.79	2.76	5.44	22.26	17.93	10.23	58.14	123.60	11.00

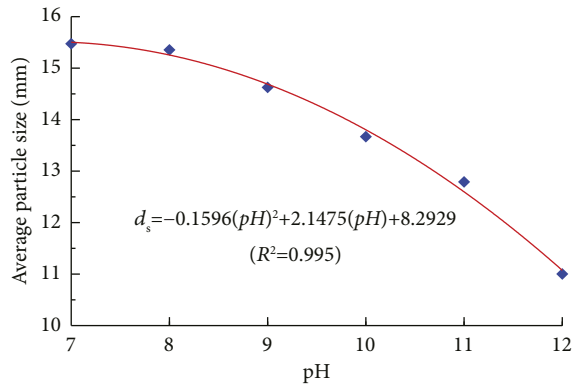

Figure 12: Variation of average particle size of sandstone specimens' fractions with pH.

the integrity of the specimen decreased, and both fracture plane and fragments increased significantly. As the solution pH reached 12, the fragmentation pattern in specimens was mainly small-sized fragments.

Study the extent of damage in rock specimens subjected to dynamic load impact based on quantitative analysis. The average particle size of the fragment's d_s [31] was taken as

$$d_s = \frac{\sum(r_i d_i)}{\sum r_i}, \tag{11}$$

where d_i represents the diameter with different grades of sieve holes, mm, and r_i represents the percentage of mass of crushed pieces relative to d_i.

According to China GB/T14685-2011 "pebbles and gravel for construction" and GB/T14684-2011 "sand for construction," 0.15, 0.3, 0.6, 1.18, 2.36, 4.75, 9.5, 13.2, and 16.0 mm square hole sand and gravel sieves were selected, using Zhejiang Geotechnical Instrument Manufacturing Ltd. Produced STSJ-4 digital high-frequency vibrating sieve machine to test pieces of broken pieces of sieving and use the balance to weigh the mass of its broken pieces under different sieve holes. The statistics of the sieving experimental results are summarized in Table 2. The variation in average particle size of sandstone specimens in dynamic compression test fragments after corrosion with different pH solutions versus pH is shown in Figure 12.

As it is shown in Figure 12, the average particle size of fragments after impact decreases as a quadratic polynomial when the pH increases, i.e., the more alkaline the solution is, the more serious the corrosion damage of the sandstone specimen is, which results in the aggravation of the impact damage to the specimen and the smaller the average grain diameter size of the fragments.

4. Conclusions

For the purpose of studying the dynamic mechanical property changes of sandstone corroded by alkaline solutions, solutions with pH 7~12 were prepared to corrode the sandstone specimens, and then, the dynamic impact compression test under the same air pressure was carried out using the SHPB device, and the resulting specimens were sieved to obtain the following three conclusions:

(1) As corrosion time extends, the pH value of strong alkali solution (pH = 11,12) decreases continuously and tends to be neutral; the pH value of weak alkali solution (pH = 8) increases slightly; the alkaline solution and neutral aqueous solution with pH 9 and 10 change less and are relatively stable.

(2) With the increase of solution pH, σ_d and E_d of sandstone corroded specimens presented varying extent of deterioration, with a maximum decrease of 17.11% and 38.45%, respectively, and ε_d as well as $\dot{\varepsilon}$ increased accordingly. Among them, the kinetic macroscopic parameters of the specimens deteriorated the most after the corrosion of strong alkali solution and the least after the corrosion of neutral solution.

(3) The effect of chemical corrosion on sandstone specimens was strengthened with the rise of solution pH. The larger the pH, the more serious the impact damage. The average particle size of specimen fragments was also reduced, and the average particle size of fragments showed a quadratic polynomial decreasing relationship with the rise of solution pH value.

In this study, only the air pressure of 0.5 MPa was used for the impact compression experiment of sandstone under corrosion, while strain-rate effects are commonly found in the kinetic properties of rocks, so in-depth research and analysis are still needed in the subsequent tests.

Data Availability

The data supporting the results of this study can be obtained from the corresponding author upon request.

Conflicts of Interest

The authors declare that there are no conflicts of interest with the publication of this paper.

Acknowledgments

This research was funded by the National Natural Science Foundation of China (nos. 52074005 and 52074006), Anhui Provincial Natural Science Foundation (no. 1808085ME134), Anhui Postdoctoral Science Foundation (no. 2015B058), and Anhui University of Science and Technology Graduate Innovation Fund Project (no. 2021CX2032). The authors thank the Engineering Research Center of Underground Mine Construction, Ministry of Education, and Anhui University of Science and Technology, State Key Laboratory of Mining Response and Disaster Prevention and Control in Deep Coal Mine, for providing the experiment conditions.

References

[1] C. B. Zhou, Y. F. Chen, Q. H. Jiang, and W Lu, "On generalized multi-field coupling for fractured rock masses and its application to rock engineering," *Chinese Journal of Rock Mechanics and Engineering*, vol. 27, no. 7, pp. 1329–1340, 2008.

[2] Y. S. Liu, X. H. Diao, and Z. L. Chen, "Dynamic mechanical properties of surrounding rock under chemical corrosion," *Journal of Nanjing Forestry University (Natural Sciences Edition)*, vol. 38, no. 6, pp. 175–178, 2014.

[3] Q. Ping, M. J. Wu, and P. Yuan, "Experimental study on dynamic mechanical properties of high temperature sandstone under impact loads," *Chinese Journal of Rock Mechanics and Engineering*, vol. 38, no. 4, pp. 782–792, 2019.

[4] X. N. Li, X. Y. Wu, and S. M. Gao, "Experiment study on uniaxial compression acoustic emission characteristics of red-bed soft rock in chemical environment," *Journal of Railway Science and Engineering*, vol. 12, no. 6, pp. 1336–1340, 2015.

[5] Y. K. Fu, Y. K. Yang, and Y. K. Guo, "Corrosion mechanism of lamprophyre under water chemistry," *Journal of Taiyuan University of Technology*, vol. 51, no. 3, pp. 404–410, 2020.

[6] R. K. Huo, F. Han, and S. G. Li, "Experimental study on physicochemical and mechanical properties of acid-corroded sandstone," *Journal of Xi'an University of Architecture and Technology*, vol. 51, no. 1, pp. 21–26, 2019.

[7] W. X. Ding, J. P. Chen, and T. Xu, "Mechanical and chemical characteristics of limestone during chemical erosion," *Rock and Soil Mechanics*, vol. 36, no. 7, pp. 1825–1830, 2015.

[8] S. X. Ling, X. Y. Wu, and C. W. Sun, "Experimental study of chemical damage and mechanical deterioration of black shale due to water-rock chemical action," *Journal of Experimental Mechanics*, vol. 31, no. 4, pp. 511–524, 2016.

[9] S. J. Miao, M. F. Cai, and D. Ji, "Damage effect of granite's mechanical properties and parameters under the action of acidic solutions," *Journal of China Coal Society*, vol. 41, no. 4, pp. 829–835, 2016.

[10] L. F. Shen, X. T Feng, and P. Z. Pan, "Experimental research on mechano-hydro-chemical coupling of granite with single fracture," *Chinese Journal of Rock Mechanics and Engineering*, vol. 29, no. 7, pp. 1379–1388, 2010.

[11] Q. Zhou and Y. L. Chen, "The experimental study on mechanical properties of granite after acid solution corrosion," *Journal of Water Resources and Water Engineering*, vol. 29, no. 1, pp. 225–231, 2018.

[12] W. Yuan, X. R. Liu, and Y. Fu, "Chemical thermodynamics and chemical kinetics analysis of sandstone dissolution under the action of dry-wet cycles in acid and alkaline environments," *Bulletin of Engineering Geology and the Environment*, vol. 78, no. 2, pp. 793–801, 2019.

[13] X. X. Liu, Y. Li, and Z. J. Fan, "Research on energy evolution and failure characteristics of single fissure carbonaceous shale under drying-wetting cycles," *Rock and Soil Mechanics*, vol. 43, no. 7, pp. 1–12, 2022.

[14] L. Y. Yu, Z. Q. Zhang, and J. Y. Wu, "Experimental study on the dynamic fracture mechanical properties of limestone after chemical corrosion," *Theoretical and Applied Fracture Mechanics*, vol. 108, 2020.

[15] Q. Ping, M. J. Wu, and Q. Y. Ma, "Comparison and analyses on reasonable loading waveform in SHPB experiment," *Chinese Journal of Underground Space and Engineering*, vol. 13, no. 6, pp. 1499–1505, 2017.

[16] M. Li, L. Qiao, and Q. W. Li, "Energy dissipation analysis of precast single jointed rock SHPB splitting test under high strain rate," *Journal of Engineering*, vol. 39, no. 7, pp. 1336–1343, 2017.

[17] P. Yuan and R. Q. Ma, "Split Hopkinson pressure bar tests and analysis of coal mine sandstone with various moisture contents," *Chinese Journal of Rock Mechanics and Engineering*, vol. 34, no. S1, pp. 2888–2893, 2015.

[18] G. L. Li, L. Y. Yu, and H. J. Su, "Dynamic properties of corroded limestone based on SHPB," *Chinese Journal of Rock Mechanics and Engineering*, vol. 37, no. 9, pp. 2075–2083, 2018.

[19] Z. Q. Zhang, L. Y. Yu, and G. L. Li, "Experimental research on dynamic tensile mechanics of limestone after chemical corrosion," *Chinese Journal of Geotechnical Engineering*, vol. 42, no. 6, pp. 1151–1158, 2020.

[20] S. S. Li, L. Y. Yu, and G. L. Li, "Experimental study on dynamic tensile strength of limestone after acid corrosion," *Jiangsu Construction*, vol. 6, pp. 88–92, 2018.

[21] Q. Ping, C. Wang, Q. Gao et al., "Experimental study on dynamic mechanical properties of sandstone corroded by strong alkali," *Applied Sciences*, vol. 12, no. 15, p. 7635, 2022.

[22] G. L. Feng, X. T. Feng, Y. X. Xiao et al., "Characteristic microseismicity during the development process of intermittent rockburst in a deep railway tunnel," *International Journal of Rock Mechanics and Mining Sciences*, vol. 124, Article ID 104135, 2019.

[23] Chinese Society for Rock Mechanics and Engineering, "T/CSRME 001-2019 Technical specification for testing method of rock dynamic properties [EB/OL]," 2019, http://www.ttbz.org.cn/Home/Show/10253.

[24] The National Standards Compilation Group of Peoples Republic of China, *GB/T 2 3561-2 010 Methods for Determining the Physical and Mechanical Properties of Coal and Rock*, Standards Press of China, Beijing, China, 2010.

[25] X. B. Li and D. S. Gu, *Rock Impact Dynamics*, pp. 2–93, Central South University of Technology Press, Changsha, China, 1994.

[26] L. L. Wang, *Foundation of Stress Waves*pp. 39–64, National Defense Industry Press, Beijing, China, 2nd edition, 2010.

[27] X. Z. Feng, N. Qin, and L. Z. Cui, "Experimental study on triaxial creep and fine view damage of sandstone under the action of water-chemical-freeze-thaw cycles," *Chinese Journal of Applied Mechanics*, vol. 38, no. 4, pp. 1383–1391, 2021.

[28] P. Wang, *Impact of Chemistry- Temperature- Stress Coupling on Mechanical Properties of Rocks*, University of Shanghai for Science and Technology, China, Shang Hai Shi, 2014.
[29] N. Zhang, S. B. Wang, and C. G. Yan, "Pore structure evolution of hydration damage of mudstone based on NMR technology," *Journal of China Coal Society*, vol. 44, no. S1, pp. 139–146, 2019.
[30] T. L. Han, J. P. Shi, and Y. S. Chen, "Laboratory investigations on the mechanical properties degradation of sandstone under the combined action between water chemical corrosion and freezing and thawing cycles," *Journal of Hydraulic Engineering*, vol. 47, no. 5, pp. 644–655, 2016.
[31] Q. Ping, C. L. Zhang, and H. J. Sun, "Experimental study on dynamic characteristics of sandstone after different high temperature cyclings," *Journal of Mining & Safety Engineering*, vol. 38, no. 5, pp. 1015–1024, 2021.